Medicine in Novel Technology and Devices 18 (2023) 100223

Contents lists available at ScienceDirect

Medicine in Novel Technology and Devices

journal homepage: www.journals.elsevier.com/medicine-in-novel-technology-and-devices/

Short Communication

Efficient calculation of fluid-induced wall shear stress within tissue engineering scaffolds by an empirical model

Husham Ahmed [a,1], Matthew Bedding-Tyrrell [a,1], Davide Deganello [b], Zhidao Xia [c], Yi Xiong [d], Feihu Zhao [a,*]

[a] Zienkiewicz Centre for Computational Engineering and Department of Biomedical Engineering, Faculty of Science & Engineering, Swansea University, Swansea, SA1 8EN, UK
[b] Welsh Centre for Printing and Coating, Faculty of Science and Engineering, Swansea University, Swansea, SA1 8EN, UK
[c] Centre for Nanohealth, Swansea University Medical School and Faculty of Medicine, Health and Life Science, Swansea University, Swansea, SA3 5AU, UK
[d] School of System Design and Intelligent Manufacturing, Southern University of Science and Technology, Shenzhen, 518055, China

ARTICLE INFO

Keywords:
Wall shear stress
Permeability
Empirical model
Tissue engineering scaffold
Bioreactor

ABSTRACT

Mechanical stimulation, such as fluid-induced wall shear stress (WSS), is known that can influence the cellular behaviours. Therefore, in some tissue engineering experiments *in vitro*, mechanical stimulation is applied via bioreactors to the cells in cell culturing to study cell physiology and pathology. In 3D cell culturing, porous scaffolds are used for housing the cells. It is known that the scaffold porous geometries can influence the scaffold permeability and internal WSS in a bioreactor (such as perfusion bioreactor). To calculate the WSS generated on cells within scaffolds, usually computational fluid dynamics (CFD) simulation is needed. However, the limitations of the computational method for WSS calculation are: (i) the high time cost of the CFD simulation (in particular for the highly irregular geometries); (ii) accessibility to the CFD model for some cell culturing experimentalists due to the knowledge gap. To address these limitations, this study aims to develop an empirical model for calculating the WSS based on scaffold permeability. This model can allow the tissue engineers to efficiently calculate the WSS generated within the scaffold and/or determine the bioreactor loading without performing the computational simulations.

1. Introduction

Mechanical stimulation, such as fluid-induced wall shear stress (WSS), is known that can influence the cellular behaviours, e.g., differentiation of stem cells, cellular proliferation, and mineralisation of extracellular matrix (ECM) [1]. To study cellular physiology and pathology in cell culturing, WSS is applied to cells via bioreactors, such as perfusion bioreactor. In tissue engineering (TE) experiments *in vitro*, cells are usually cultured in a 3D environment, for which porous scaffolds are used for housing the cells [2]. Previous studies have found that scaffold porous geometric characteristics, such as porosity, pore size and pore shape, can influence the internal microfluidic environment, including the WSS on cells within scaffolds [3,4]. Also, according to Refs. [3,5], porous geometric characteristics can influence the scaffold permeability, which affects the nutrient delivery within the scaffold.

To quantify the WSS within scaffold, usually a numerical approach (e.g., based on computational fluid dynamics – CFD model) is needed due to the infeasibility of direct measurement of fluid-induced WSS [4,6]. These CFD models are based on the scaffold geometries from either computer-aided design (CAD) [5,7] or micro-computed tomography (microCT) images [7,8]. However, there are a few limitations of WSS calculation. Firstly, for cell culturing experimentalists, the accessibility to the CFD model is limited due to the knowledge gap [2]. Therefore, they need the help from computational engineers for calculating the WSS and/or determining the applied loading to the bioreactors. Secondly, if the CFD simulation is based on the scaffold geometry from CAD, it is likely that the calculated WSS would have a deviation from the real WSS in the manufactured scaffold due to the manufacturing error, according to the findings in previous study [7]. Thirdly, if the CFD model is based on the scaffold geometry that reconstructed from microCT images, the

* Corresponding author. Zienkiewicz Centre for Computational Engineering and Department of Biomedical Engineering, Faculty of Science & Engineering, Swansea University, Bay Campus, Swansea, SA1 8EN, UK.
E-mail address: feihu.zhao@swansea.ac.uk (F. Zhao).
[1] These authors contributed equally to this paper.

https://doi.org/10.1016/j.medntd.2023.100223
Received 21 December 2022; Received in revised form 22 February 2023; Accepted 4 March 2023

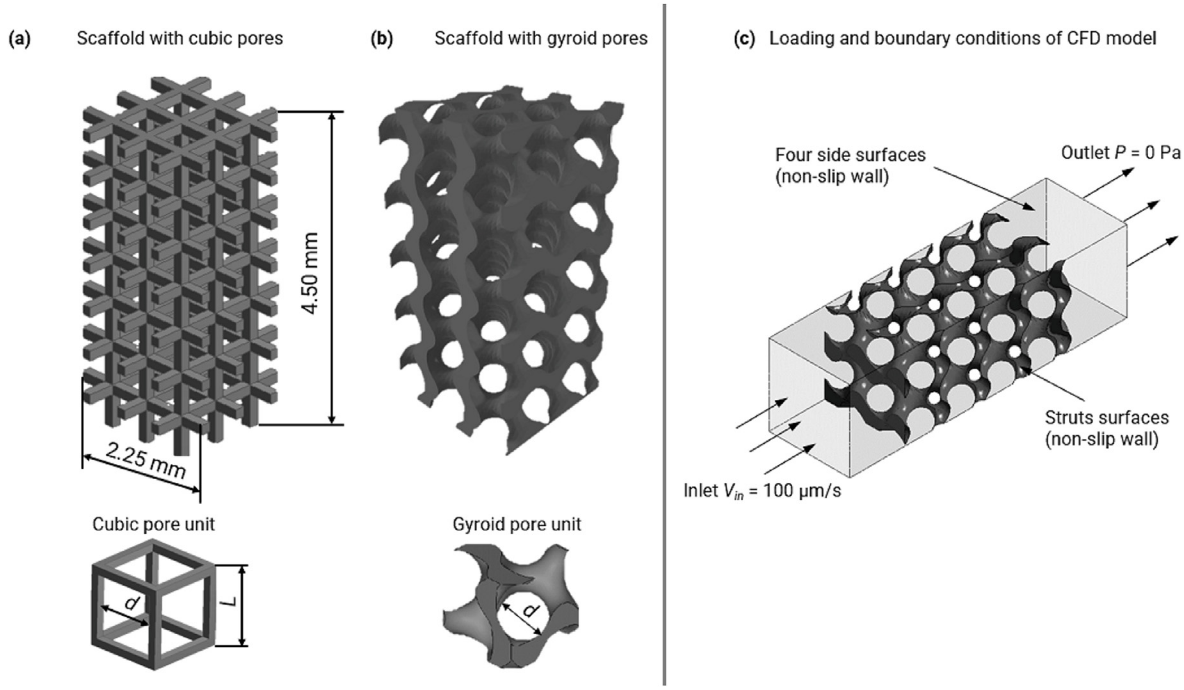

Fig. 1. Porous scaffold geometries with **(a)** cubic pore unit (i.e., symmetric pore shape) and **(b)** gyroid pore unit (i.e., non-symmetric pore shape); **(c)** illustration of boundary and loading conditions of the CFD model.

computational time cost could be high, in particular for the scaffold with highly irregular struts geometries [9]. Furthermore, the WSS would change with the tissue growth inside the scaffold [10]. To determine the real-time adjustment/optimisation of the bioreactor loading, a more advanced computational model, which couples the tissue growth within scaffold and the CFD model is needed, such as [10–12]. However, the time cost will be even higher to run these advanced computational models.

To address these limitations, it is hypothesised that a simple empirical model for correlating the scaffold internal WSS and permeability exists. If the hypothesis is true, this empirical model will allow the tissue engineers/bioreactor users to easily calculate the WSS generated within the scaffold and/or tune the bioreactor loading without performing the numerical simulations.

2. Methods

2.1. Scaffold geometry generation

To generate the data of WSS and permeability, the scaffolds with two types of pore shapes were proposed, cubic shape and gyroid shape, which represented (i) symmetric pore unit and (ii) non-symmetric pore unit, respectively. The scaffolds with cubic and gyroid pore shapes have been commonly used for *in vitro* and *in vivo* TE with the application of accurate 3D printing technique in scaffold manufacturing [13]. The investigated pore size d and porosity φ are in the ranges of 300–1000 μm and 60%–90% respectively, which were typically seen in TE applications [2].

The scaffolds with cubic pores were created in SolidWorks (Dassault Systèmes, France) using Eq. (1) for controlling the pore size (d) and porosity (φ) [14]:

$$\varphi = -2\left(\frac{d}{L}\right)^3 + 3\left(\frac{d}{L}\right)^2 \tag{1}$$

where, L is the length of the repeating unit (Fig. 1a).

The scaffolds with gyroid (i.e., triply periodic minimal surfaces - TPMS) pore geometries were created in an open-source software, MSLattice [15]. To generate the gyroid pores with controlled the pore size and porosity, the level set method was applied on the implicit function of gyroid topology (Eq. (2) [16]):

$$\sin(x)\cos(y) + \sin(z)\cos(x) + \sin(y)\cos(z) - C = 0 \tag{2}$$

where x, y and z were the coordinates, C was the level constant that was defined by Walker et al. in Eqs. (3) and (4) [16]:

$$C = 0.7864\varphi^3 - 1.1798\varphi^2 - 2.5259\varphi + 1.4597 \tag{3}$$

$$d = -11.7311C^5 - 0.1307C^4 - 1.7987C^3 + 0.2070C^2 - 186.9928C + 433.0114 \tag{4}$$

Therefore, C was associated with porosity φ and pore size d for generating the gyroid geometry with defined porosity and pore size in MSLattice [15].

All these geometries were imported to ANSYS – CFX (ANSYS Inc, PA, USA) for CFD simulation as illustrated in supplementary material.

2.2. CFD simulation

To calculate the scaffold permeability and internal WSS, the CFD approach will be used. The scaffold permeability (κ) describes how easily the medium/liquid can move through. It can be calculated according to Darcy's law:

$$\kappa = \frac{Q \cdot \mu \bullet H}{A \bullet \Delta P} \tag{5}$$

where, Q is the prescribed flow rate; A is the cross-sectional area to flow; μ is the dynamic viscosity of the medium (similar as water $\mu = 0.889$ mPa s [17]); ΔP is the pressure drop over the scaffold length H ($H = 4.5$ mm), ΔP is calculated from CFD simulation.

The WSS on the scaffold surface (Γ_S) was calculated according to Eq. (6) from CFD model:

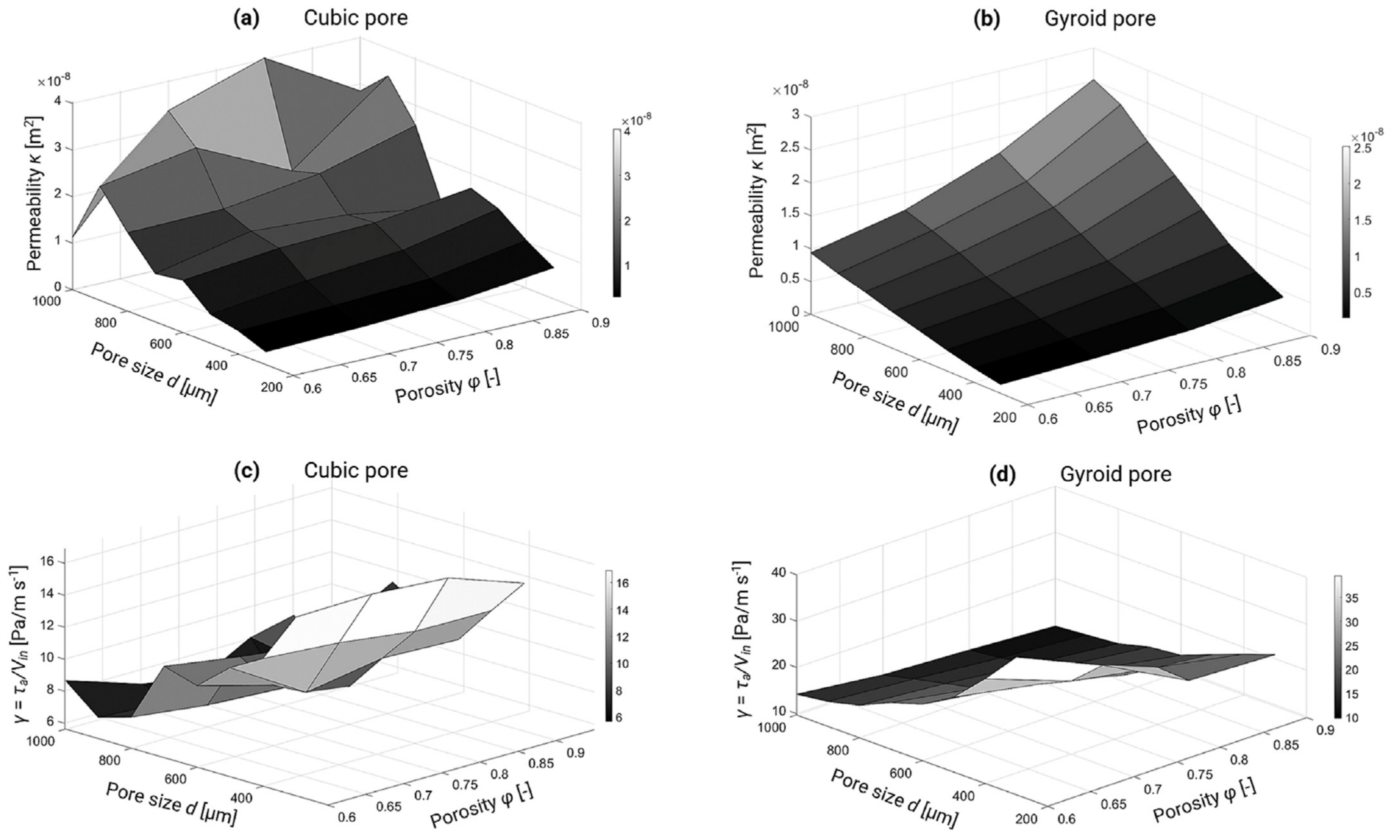

Fig. 2. Scaffold permeability of **(a)** cubic pores and **(b)** gyroid pores influenced by pore size and porosity; ratio of average WSS (τ_a) and applied fluid velocity (V_{in}) of **(c)** cubic pores and **(d)** gyroid pores influenced by pore size and porosity.

$$\tau_{ij} = \mu\left(\frac{\partial v_i}{\partial x_j} + \frac{\partial v_j}{\partial x_i}\right)\bigg|_{x_i \in \Gamma_S} \tag{6}$$

where, x_i (or x_j) is the ith (or jth) spatial coordinates.

In the CFD model, considering the application context of perfusion bioreactor in TE, we applied the inlet fluid velocity of 100 μm/s [14], and outlet relative pressure of 0 Pa (i.e., atmospheric pressure) in Fig. 2. The culturing medium simulated in this study had the same properties as water, i.e., density $\rho = 1000$ kg/m. According to the pre-computation in ANSYS – CFX, the maximum Reynolds number was 0.54 among all the geometries, manifesting the flow was laminar. The side surfaces and struts surfaces were defined as non-slip walls (i.e., the fluid has zero velocity relative to the solid surfaces) as shown in Fig. 2. After mesh sensitivity analysis, the model geometry was mesh by 375 μm, and the mesh element size for all the non-slip walls (pointed out in Fig. 1c) was refined to 37.5 μm. The mesh captured curvature features of the geometries, i.e., the maximum allowable angle that one element edge could span another was 18°. The mesh was generated by a quadratic tetrahedron method with a patch conforming algorithm. The CFD model was solved using finite volume method by ANSYS – CFX under the convergence criteria of the root mean square residual of the mass and momentum $<10^{-4}$.

2.3. Regression analysis

To obtain the correlation between the permeability (κ) and average value of WSS (τ_a), regression analysis was carried out on κ and τ_a of different scaffold geometries under the 95% confidence interval. As two scaffold pore shapes in this study (cubic and gyroid) represented the symmetric pore unit and non-symmetric pore unit, the regression analysis was conducted on each pore shapes separately.

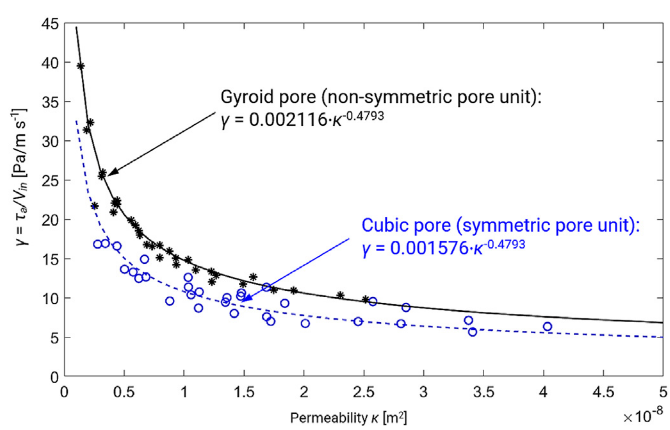

Fig. 3. Empirical model based on the power-law function for correlating the average WSS and permeability (blue o and - - are the CFD simulation data and fitted function for cubic pore shape; black * and – are the CFD simulation data and fitted function for gyroid pore shape). (For interpretation of the references to colour in this figure legend, the reader is referred to the Web version of this article.)

3. Results

As the average WSS was proportional to the inlet fluid velocity [14, 18,19], we introduced a parameter $\gamma = \tau_a/V_{in}$ for WSS characterisation. It was found that the permeability and WSS both were dependent on the porosity, pore size and pore shape (Fig. 2). The permeability and WSS increased with the decreasing of porosity and pore size, although some anomalies were observed in cubic pore (Fig. 2a).

	Scaffolds that have non-symmetric pore units		Scaffolds that have symmetric pore units	
	Irregular pores Type 1	Irregular pores Type 2	Spherical pores	Cubic pores
	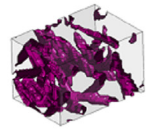	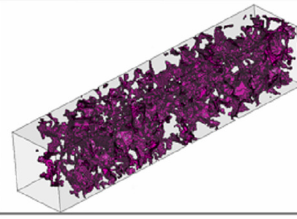	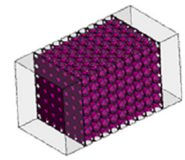	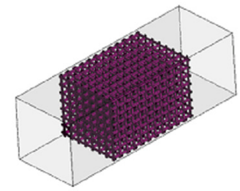
κ	7.8×10^{-11} m^2	3.9×10^{-10} m^2	1.3×10^{-9} m^2	5.3×10^{-10} m^2
V_{in}	100 μm/s			
Predicted τ_a	13.7 mPa	6.8 mPa	2.8 mPa	4.4 mPa
CFD τ_a	14.8 mPa	5.9 mPa	2.3 mPa	4.1 mPa

Fig. 4. Verification of the empirical model using the irregular pores (representing the scaffolds without symmetric pore unit); and the regular pores with spherical and cubical shapes (representing the scaffolds with symmetric repeating pore unit).

The data showed the nonlinear trend between the permeability κ and parameter γ as shown in Fig. 3. Therefore, nonlinear regression, which was based on the power-law function was used in Matlab (MathWorks, CA, USA). Finally, an analytical function with the different coefficient values was derived as below:

$$\gamma = A \bullet \kappa^{-0.4793} \tag{7}$$

where, A is the coefficient, $A = 0.002116$ for gyroid pore shape (non-symmetric pore unit) with the R-square $= 0.9598$; $A = 0.001576$ for cubic pore shape (symmetric pore unit) with the R-square $= 0.7824$.

4. Discussion and conclusion

In this study, a simple empirical model, which can correlate the scaffold permeability with the resultant average WSS was developed.

The Kozeny – Carman equation showed that the permeability is dependent on the porosity, struts size and shape [20]. The results of permeability (in Fig. 2 a and b) agreed with the trend of the permeability change predicted by the Kozeny-Carman equation. Also, the influence of pore size and porosity on the WSS observed in this study (Fig. 2 c and d) was similar as that reported in Ref. [14]. For cubic pore geometry, the anomalies of κ (Fig. 2a) and γ (Fig. 2c) were due to the imperfect pores in the region close to the boundaries (e.g. 4 side faces) when fitting the repeating pore units into a confined volume. However, this influence was trivial for gyroid pore geometry. Therefore, to reduce the influence that might be caused by the anomalies of the data, we firstly applied the nonlinear regression to the data of gyroid pore (black * in Fig. 3) to obtain Eq. (7). Afterwards, this equation with an already determined exponent of −0.4793 was applied to the data of cubic pore (blue o in Fig. 3) for determining the coefficient C.

To verify the accuracy of this empirical model, we tested it with 4 different geometries, which have been used in TE applications (Fig. 4). The scaffolds with non-symmetric pore units (irregular pore shapes) are usually made by electrospinning / salt leaching [21,22]; while the symmetric pore units (spherical and cubic pore shapes) can be fabricated by various techniques (such as: salt leaching / sintering / 3D printing [23–25]). The WSS was calculated using Eq. (6) based on CFD approach. It was found that the average error of prediction by empirical model was 11.3% for scaffolds with non-symmetric pore units (irregular pore shapes); 14.5% for scaffolds assembled by symmetric pore units (spherical and cubic pore shapes). Therefore, it has been demonstrated that this empirical model has reasonable accuracy in WSS calculation for the scaffold geometries investigated/tested in this study. Also, it is expected that this empirical model can be applied on other scaffolds, which have (i) non-symmetric pore units (such as: irregular pore shapes, TPMS structures with Schwarz D/P pore shapes, etc.); (ii) symmetric pore units (such as: cylindrical, prism and diamond pore shapes, etc.). For further improving the empirical model accuracy, more scaffolds with various porous geometries need to be tested in the future work.

In conclusion, a power-law based empirical model was developed, for the first time, for calculating the average WSS within scaffolds according to the permeability. The researchers can easily use it for rapidly determining the mechanobiological experiment conditions for TE *in vitro* without performing computational simulations, e.g., quantifying the resultant WSS on cells within scaffolds and/or determining the applied loading (such as flow rate) to the bioreactor.

Funding

This study was supported by the Royal Society Research Grant (reference code: RGS/R2/212,280) and Swansea University IMPACT – Green Recovery funding. Matthew Bedding-Tyrrell is supported by EPSRC – Doctoral Training Partnership (DTP) scholarship (reference code: EP/T517987/1 - 2573181)

Author contribution

Husham Ahmed: Methodology, Software, Investigation, Writing. Matthew Bedding-Tyrrell: Methodology, Software, Investigation, Writing. Davide Deganello: Reviewing and Editing. Zhidao Xia: Reviewing and Editing. Yi Xiong: Conceptualization, Reviewing and Editing. Feihu Zhao: Conceptualization, Reviewing, Editing and Revising, Supervision

Declaration of competing interest

None

Appendix A. Supplementary data

Supplementary data to this article can be found online at https://doi.org/10.1016/j.medntd.2023.100223.

References

[1] Delaine-Smith RM, Reilly GC. Mesenchymal stem cell responses to mechanical stimuli. Muscles Ligaments Tendons J 2012;2:169–80.

[2] Zhao F, Xiong Y, Ito K, van Rietbergen B, Hofmann S. Porous geometry guided micro-mechanical environment within scaffolds for cell mechanobiology study in bone tissue engineering. Front Bioeng Biotechnol 2021;9:1–10. https://doi.org/10.3389/fbioe.2021.736489.

[3] Ali D, Sen S. Finite element analysis of mechanical behavior, permeability and fluid induced wall shear stress of high porosity scaffolds with gyroid and lattice-based architectures. J Mech Behav Biomed Mater 2017;75:262–70. https://doi.org/10.1016/j.jmbbm.2017.07.035.

[4] Pires T, Dunlop JWC, Fernandes PR, Castro APG. Challenges in computational fluid dynamics applications for bone tissue engineering. Proc R Soc A: Math Phys Eng Sci 2022;478. https://doi.org/10.1098/rspa.2021.0607.

[5] Castro APG, Pires T, Santos JE, Gouveia BP, Fernandes PR. Permeability versus design in TPMS scaffolds. Materials 2019;12. https://doi.org/10.3390/ma12081313.

[6] Sanz-Herrera JA, Reina-Romo E. Continuum modeling and simulation in bone tissue engineering. Appl Sci 2019;9. https://doi.org/10.3390/app9183674.

[7] Marin AC, Lacroix D. The inter-sample structural variability of regular tissue-engineered scaffolds significantly affects the micromechanical local cell environment. Interface Focus 2015;5. https://doi.org/10.1098/rsfs.2014.0097.

[8] Zhao F, Melke J, Ito K, van Rietbergen B, Hofmann S. A multiscale computational fluid dynamics approach to simulate the micro-fluidic environment within a tissue engineering scaffold with highly irregular pore geometry. Biomech Model Mechanobiol 2019;18:1965. https://doi.org/10.1007/s10237-019-01188-4. –77.

[9] Zermatten E, Vetsch JR, Ruffoni D, Hofmann S, Müller R, Steinfeld A. Micro-computed tomography based computational fluid dynamics for the determination of shear stresses in scaffolds within a perfusion bioreactor. Ann Biomed Eng 2014;42: 1085–94. https://doi.org/10.1007/s10439-014-0981-0.

[10] Guyot Y, Papantoniou I, Luyten FP, Geris L. Coupling curvature-dependent and shear stress-stimulated neotissue growth in dynamic bioreactor cultures: a 3D computational model of a complete scaffold. Biomech Model Mechanobiol 2016;15: 169–80. https://doi.org/10.1007/s10237-015-0753-2.

[11] Nava MM, Raimondi MT, Pietrabissa R. A multiphysics 3D model of tissue growth under interstitial perfusion in a tissue-engineering bioreactor. Biomech Model Mechanobiol 2013;12:1169–79. https://doi.org/10.1007/s10237-013-0473-4.

[12] Castro APG, Lacroix D. Micromechanical study of the load transfer in a polycaprolactone–collagen hybrid scaffold when subjected to unconfined and confined compression. Biomech Model Mechanobiol 2018;17:531–41. https://doi.org/10.1007/s10237-017-0976-5.

[13] Dong Z, Zhao X. Application of TPMS structure in bone regeneration. Eng Regen 2021;2:154–62. https://doi.org/10.1016/j.engreg.2021.09.004.

[14] Zhao F, Vaughan TJ, McNamara LM. Quantification of fluid shear stress in bone tissue engineering scaffolds with spherical and cubical pore architectures. Biomech Model Mechanobiol 2016;15:561–77. https://doi.org/10.1007/s10237-015-0710-0.

[15] Al-Ketan O, Abu Al-Rub RK. MSLattice: a free software for generating uniform and graded lattices based on triply periodic minimal surfaces. Mater Des Process Commun 2021;3:1–10. https://doi.org/10.1002/mdp2.205.

[16] Walker JM, Bodamer E, Kleinfehn A, Luo Y, Becker M, Dean D. Design and mechanical characterization of solid and highly porous 3D printed poly(propylene fumarate) scaffolds. Prog Addit Manuf 2017;2:99–108. https://doi.org/10.1007/s40964-017-0021-3.

[17] Poon C. Measuring the density and viscosity of culture media for optimized computational fluid dynamics analysis of in vitro devices. J Mech Behav Biomed Mater 2022;126:105024. https://doi.org/10.1016/j.jmbbm.2021.105024.

[18] Mccoy RJ, Jungreuthmayer C, O'Brien FJ. Influence of flow rate and scaffold pore size on cell behavior during mechanical stimulation in a flow perfusion bioreactor. Biotechnol Bioeng 2012;109:1583–94. https://doi.org/10.1002/bit.24424.

[19] Lesman A, Blinder Y, Levenberg S. Modeling of flow-induced shear stress applied on 3D cellular scaffolds: implications for vascular tissue engineering. Biotechnol Bioeng 2009;105:645–54. https://doi.org/10.1002/bit.22555.

[20] Kruczek B. Carman–kozeny equation. In: Drioli E, Giorno L, editors. Encyclopedia of membranes. Berlin, Heidelberg: Springer; 2015. p. 1–3.

[21] Melke J, Midha S, Ghosh S, Ito K, Hofmann S. Silk fibroin as biomaterial for bone tissue engineering. Acta Biomater 2016;31:1–16. https://doi.org/10.1016/j.actbio.2015.09.005.

[22] Lannutti J, Reneker D, Ma T, Tomasko D, Farson D. Electrospinning for tissue engineering scaffolds. Mater Sci Eng C 2007;27:504–9. https://doi.org/10.1016/j.msec.2006.05.019.

[23] Xie Y, Hardouin P, Zhu Z, Tang T, Dai K, Lu J. Three-dimensional flow perfusion culture system for stem cell proliferation inside the critical-size b-tricalcium phosphate scaffold. Tissue Eng 2006;12:3535–43. https://doi.org/10.1089/ten.2006.12.3535.

[24] Rubert M, Rita Vetsch J, Lehtoviita I, Sommer M, Zhao F, Studart AR, et al. Scaffold pore geometry guides gene regulation and bone-like tissue formation in dynamic cultures. Tissue Eng 2020. https://doi.org/10.1089/ten.TEA.2020.0121.

[25] Egan PF. Integrated design approaches for 3D printed tissue scaffolds: review and outlook. Materials 2019;12. https://doi.org/10.3390/ma12152355.